Revealing the structure and organization of intercellular tunneling nanotubes (TNTs) by STORM imaging

Lilin Huang,† Jiao Zhang,† Zekai Wu, Liangliang Zhou, Bin Yu, Yingying Jing,* Danying Lin* and Junle Qu

Shenzhen Key Laboratory of Photonics and Biophotonics, Key Laboratory of Optoelectronic Devices and Systems of Ministry of Education and Guangdong Province, College of Physics and Optoelectronic Engineering, Shenzhen University, Shenzhen 518060, P. R. China

† These authors contributed equally to this work.

* Emails: yyjing@szu.edu.cn; dylin@szu.edu.cn

Experimental section

Cell culture

BS-C-1 cells (African green monkey kidney cell line), U2OS cells (human osteosarcoma cell line), HeLa cells (cervical cancer cell line) and KYSE150 cells (esophageal cancer cell line) were cultured in desired fresh medium (BS-C-1 cells in MEM (Procell), U2OS cells in McCoy's 5A (Macklin), BS-C-1 cells is a kind of common cell line for studying the structure and distribution of microfilaments and microtubule in cells[1-3]. The three types of cancer cells (esophageal cancer cells KYSE150, cervical cancer cells HeLa and human osteosarcoma cells U2OS) are commonly used to study the physiological and pathological processes in the laboratory[4, 5]. HeLa and KYSE150 cells in RPMI-1640 (Thermo Fisher)) containing 10% fetal bovine serum (FBS; Gibco, 10099-141) and 1% penicillin-streptomycin (Gibco, 15140122). All cells were trypsinized with 0.25% Trypsin (Gibco, 25200072) for passaging and incubated in a humidified chamber with 5% CO2 at 37°C, and the medium were replaced every 2-3 days.

Tubulin Staining

Cells were grown on a glass-bottom dish (NEST, 801001) at an appropriate density and cultured until reaching a covering rate of 60%. To improve the tubulin labelling efficient, cells were incubated with 0.5% Triton X-100 in extract solution (100 mM PIPES, 1 mM EGTA, 1 mM $MgCl_2$) at 37°C for 30 s before staining[6]. After washed in phosphate-buffered saline (PBS), cells were fixed in 4% paraformaldehyde (PFA) in extract solution described above for 10 min. Then cells were washed in PBS and incubated with freshly prepared $NaBH_4$ solution (1 mg/ml) to decrease sample-induced noise, and washed in PBS three times. Subsequently, cells were permeabilized (0.5% Triton X-100) and blocked (3% BSA) for 1h.

For tubulin immunostaining, cells were first incubated with α-Tubulin Monoclonal Antibodies (1:500; Thermo Fisher Scientific, MA1-80017) for 3 h. After washed in PBS for three times, cells were incubated for 1h with secondary Alexa Fluor™ 647 Goat anti-Rat IgG (H+L) antibodies (1:500; Thermo Fisher Scientific, A-21247) or Alexa Fluor™ 488 Donkey anti-Rat IgG (H+L) antibodies (1:500; Thermo Fisher Scientific, A-21208). Then cells were washed in PBS and post-fixed (0.5% Glutaraldehyde) for 30 min, and washed in PBS three times again.

Actin staining

For actin staining, cells were fixed (4% PFA) for 15 min at room temperature. After washed in PBS, cells were permeabilized (0.5% Triton X-100) for 10 min. Then cells were washed in PBS and blocked (3% BSA) for 45 min to block the nonspecific binding. After washed in PBS, cells were stained for 45 min with Alexa Fluor™ 647 conjugated Phalloidin (1:40; Thermo Fisher Scientific, A22287), and washed in PBS for three times.

Mitochondria staining

For Mitochondria staining, cells were washed in PBS and fixed (4% PFA) for 10 min. After washed in PBS, cells were incubated with freshly prepared $NaBH_4$ solution (1 mg/ml). Then cells were washed and incubated for 3 h with mitochondria monoclonal antibodies (1:500; Thermo Fisher Scientific, MA5-12017). This antibody recognizes a 60kDa non-glycosylated protein component of mitochondria found in normal and malignant human cells. Primary antibodies were detected using secondary Alexa Fluor™ 647 Goat anti-Mouse IgG (H+L) antibodies (1:500; Thermo Fisher Scientific, A28181). Secondary antibodies were as well incubated for 1 h at room temperature. After washed in PBS, cells were post-fixed (4% PFA) for 10 min and washed in PBS for three times.

Microscopy setup and data acquisition

Prior to performing STORM, the imaging buffer was prepared, containing 200 µl of 0.2 g/ml glucose solution, 100 µl of 1 M Tris buffer, 10 µl of 1 M NaCl solution, 10 µl β-mercaptoethanol, 10 µl oxygen scavenging system buffer (containing 0.08 g/ml glucose oxidase, 8 µg/ml Catalase in PBS), and 670 µl of deionized water.

The STORM imaging was performed on an inverted fluorescence microscope (Ti2-U, Nikon), equipping with a 100× 1.45 NA oil immersion objective lens. For single color STORM imaging, the Alexa Fluor™ 647 were excited with the 640-nm laser (640nm/500mW, MPBC-CA) and the emission was collected using a dichroic mirror (ZT640rdc, Chroma) within the microscope and a bandpass filter (ET706/95m, Chroma) prior to the detector. Fluorescent signals were collected via a cooled EMCCD camera (DU897, Andor). The laser power was held constant at 200 mW. A time series of 15,000 frames per TNT event were recorded at a rate of 30 Hz for the reconstruction of the super-resolution image.

3D-STORM imaging

For 3D-STORM imaging, a cylindrical lens with a focal length of 1000 mm was used before the EMCCD to introduce astigmatism for 3D localization[7]. An anti-drift module was performed to eliminated the axial drift of the objective lens[8]. A 785-nm laser was used as a reference light. The reference light reflected from the coverslip-sample interface was incident on the quadrant detector (QD). By detecting the lateral drift of the spot with the QD, the axial drift of objective lens can be measured and corrected with a piezo stage (FOC100, Piezoconcept). Acquisition sequences of 40,000 frames were recorded at a rate of 100 Hz with the laser power of 100 mW.

Image reconstruction

Traditional single-molecule localization algorithms were employed for data processing. Firstly, image filtering was used to eliminate the high- and low-frequency noise. Secondly, we used a nonlinear least-

squares fitting algorithm to fit a two-dimensional Gaussian model for each point spread function (PSF) to achieve single molecule localization. The model can be expressed as:

$$I(x,y) = A\exp\left[-\frac{(x-x_0)^2+(y-y_0)^2}{2\delta^2}\right]+b, \quad (1)$$

where (x_0, y_0) is the center of the PSF (i.e., the Airy disk formed by a fluorescent molecule), corresponding to the actual coordinates of the molecule on the object plane, $I(x, y)$ is the theoretical intensity at pixel (x, y), A is the peak intensity, δ is the standard deviation of the Gaussian function, representing the sized of the PSF, and b is the background noise. By fitting $I(x, y)$ to the actual intensity distribution of the detected PSF, the coordinates and the peak intensity of the molecule can be obtained. Finally, a super-resolution image was formed by listing the molecules at their positions with the peak intensities, and the width of each peak can be presented as the localization uncertainty.

3D-STORM image reconstruction

For single molecule localization in cylindrical lens-based 3D-STORM imaging, the fitting model for the deformed PSFs can be represented by an elliptic Gaussian function as:

$$I(x,y) = A\exp\left(-\frac{(x-x_0)^2}{2\delta_x^2}-\frac{(y-y_0)^2}{2\delta_y^2}\right)+b, \quad (2)$$

Where δ_x and δ_y represent the standard deviations in the x and y directions, respectively. By fitting the corrected model to an oval PSF, we can not only determine the lateral coordinates (i.e., (x_0, y_0)) of molecule, but also obtain the standard deviations for further determining the axial coordinates. Specifically, the axial information can be obtained according to the relationship between the shape of the PSF and the defocusing distance (z) of the molecule. It can be approximately expressed as[7]:

$$\delta_{x,y}(z) = \delta_0\sqrt{1+\left(\frac{z-z_1}{d}\right)^2+B\left(\frac{z-z_1}{d}\right)^3+C\left(\frac{z-z_1}{d}\right)^4}, \quad (3)$$

Where δ_0 is the standard deviation when the molecule is just in the average focal plane, z_1 is the offset of the x or y focal plane from the average focal plane, d is the focal depth of the microscope, B and C are coefficients of higher order terms used to correct non-ideality of the imaging optics. By collecting PSFs using small fluorescent beads at different known positions along z axis, we can get a calibration curve with formula (3). By compared the standard deviations δ_x and δ_y with the calibration curve, the axial position of the fluorescent molecule can be obtained, thereby realizing 3D imaging.

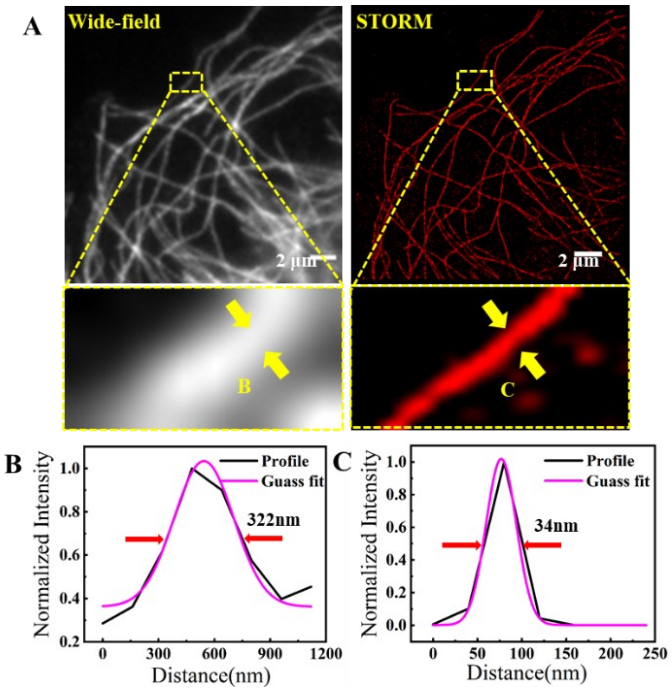

Figure S1. Evaluating the super-resolution imaging performance of the home-built STORM system. (A) Wide-field image and corresponding STORM image of microtubules in BS-C-1 cells. (B) Cross-sectional distribution of localizations generated from the data marked in (A). The red arrows show the FWHM of the Gaussian fit lines (magenta).

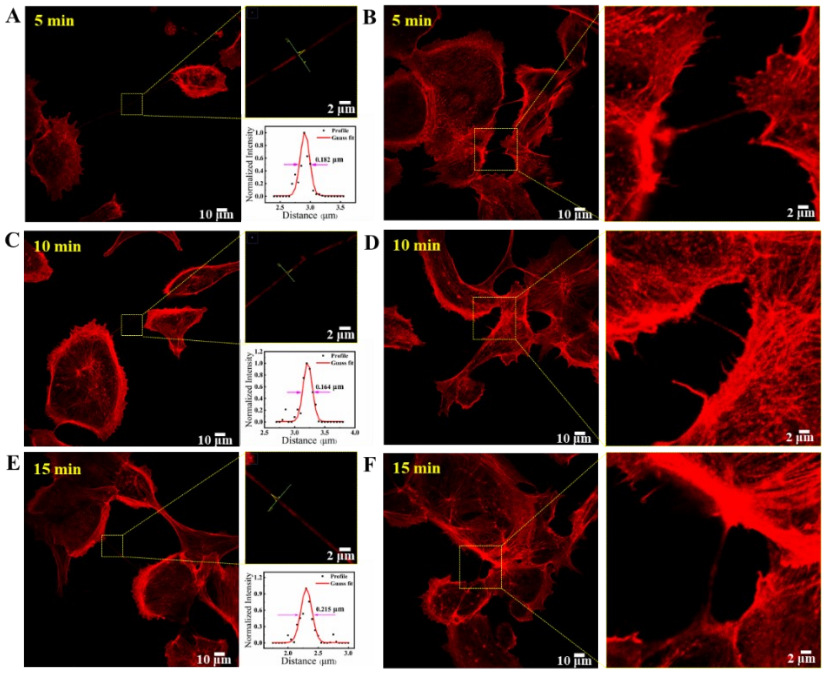

Figure S2. Representative confocal images of microfilaments in TNTs with different permeabilization times: (A-B) 5 min; (C-D) 10 min; (E-F) 15 min. Thin TNTs could be observed with different permeabilization times as shown in (A), (C), and (E). Cells were examined with Nikon A1plus confocal microscope (oil objective 60×/1.4NA).

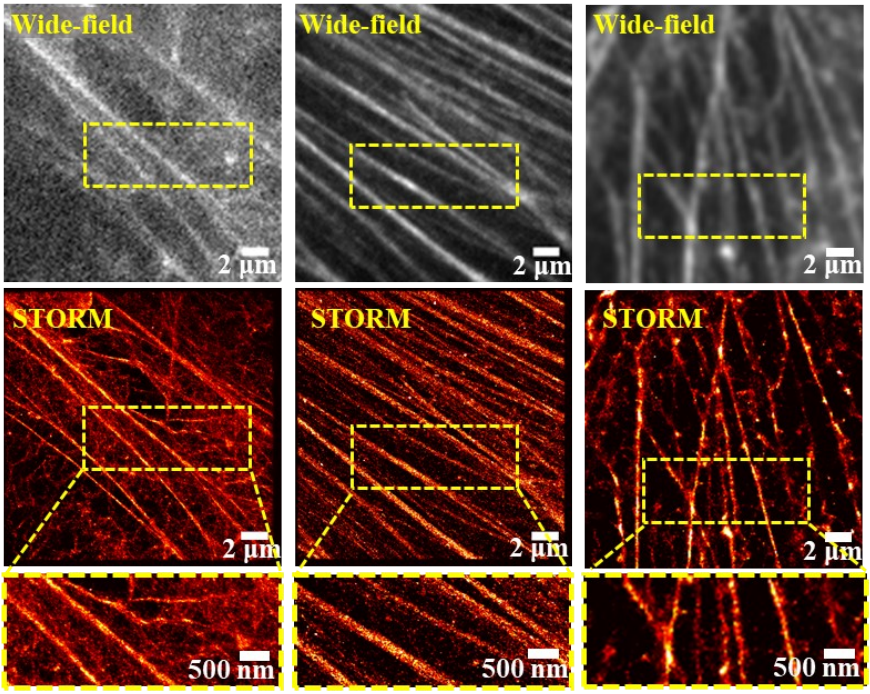

Figure S3. Representative wide-field images and corresponding STORM images of microfilaments in cells using a 10-min permeabilization time. The intracellular microfilaments could be labelled and imaged well with STORM fluorescent imaging.

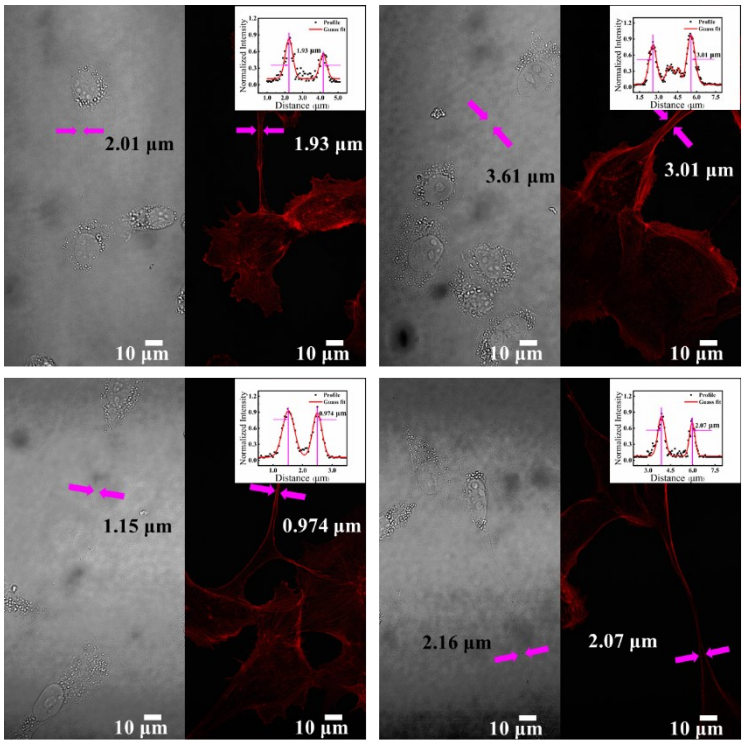

Figure S4. Comparison of the width of TNTs measured from the bright-view images with the gaps of the outermost microfilaments from the fluorescent images. The widths of TNTs from bright-view images were measured using image analysis tools in Image J. The gaps of microfilaments were measured from the corresponding cross-sectional profiles of the arrow pointing regions.

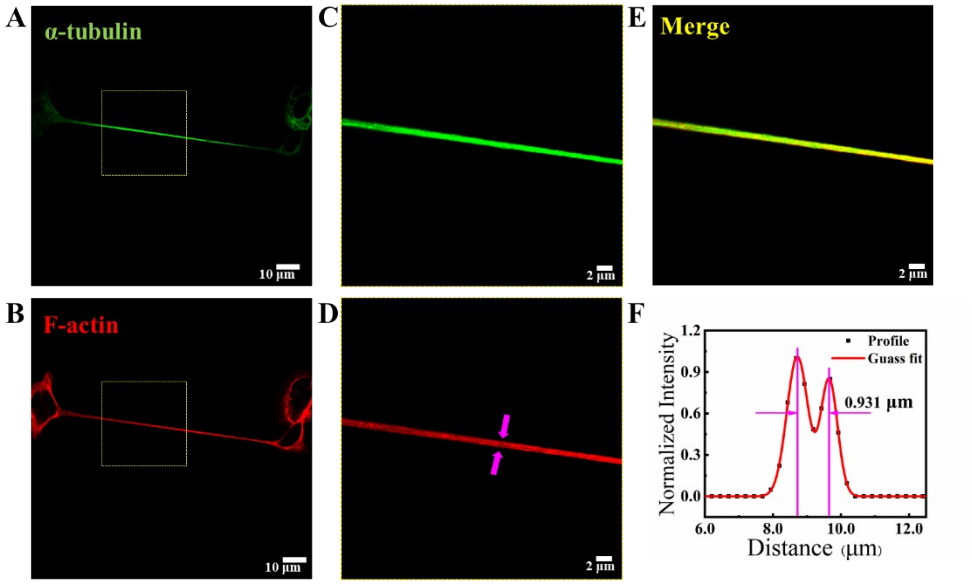

Figure S5. Dual-color confocal images reveals the relationship of microfilaments and microtubules in a TNT. (A) The tubulin was stained with primary α-Tubulin monoclonal antibodies and Alexa Fluor™ 488 conjugated secondary antibodies. (B) The F-actin was labeled with Alexa Fluor™ 647 conjugated Phalloidin. (C-D) Enlarged images of the boxed regions in (A-B). (E) Merged image of (C) and (D). (F) Corresponding cross-sectional profiles of the arrow pointing region in (D).

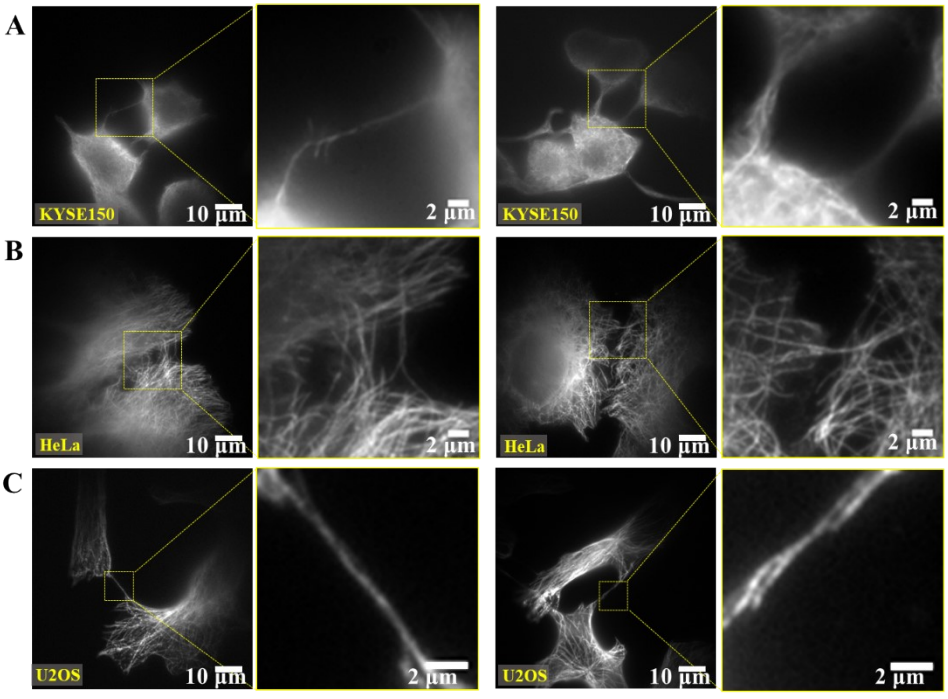

Figure S6. (A-C) Corresponding larger view of the wide-field images in Figure 2D, 2E, and 2F, respectively.

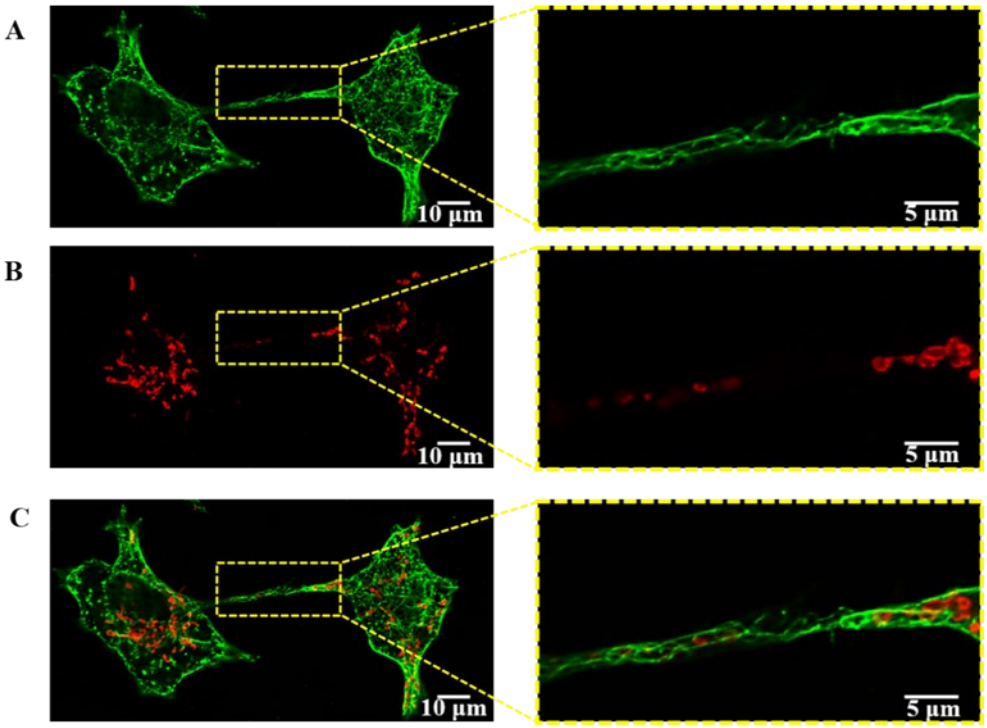

Figure S7. Dual-color confocal images reveal the relationship of microtubules (A) and mitochondria (B) in a TNT between two BS-C-1 cells. The microtubules were labelled with α-Tubulin monoclonal antibodies and Alexa Fluor™ 488 conjugated secondary antibodies, and mitochondria were labelled with primary antibodies against mitochondria (this antibody recognizes a 60kDa non-glycosylated protein component of mitochondria) and Alexa Fluor™647 conjugated antibodies. The merged image (C) shows the transfer of mitochondria via the TNT.

Notes and references

1. T. E. Hoornweg, E. M. Bouma, D. P. I. van de Pol, I. A. Rodenhuis-Zybert and J. M. Smit, *PLoS Negl. Trop. Dis.*, 2020, **14**, e0008469.
2. C. E. Park, Y. Cho, I. Cho, H. Jung, B. Kim, J. H. Shin, S. Choi, S. K. Kwon, Y. K. Hahn and J. B. Chang, *ACS Nano*, 2020, **14**, 14999-15010.
3. I. Verdeny-Vilanova, F. Wehnekamp, N. Mohan, A. Sandoval Alvarez, J. S. Borbely, J. J. Otterstrom, D. C. Lamb and M. Lakadamyali, *J. Cell Sci.*, 2017, **130**, 1904-1916.
4. K. Gousset, L. Marzo, P. H. Commere and C. Zurzolo, *J. Cell Sci.*, 2013, **126**, 4424-4435.
5. R. Mittal, E. Karhu, J. S. Wang, S. Delgado, R. Zukerman, J. Mittal and V. M. Jhaveri, *J. Cell. Physiol.*, 2019, **234**, 1130-1146.
6. A. R. Halpern, M. D. Howard and J. C. Vaughan, *Curr. Protoc. Chem. Biol.*, 2015, **7**, 103-120.
7. B. Huang, W. Wang, M. Bates and X. Zhuang, *Science*, 2008, **319**, 810-813.
8. Y. Huo, B. Cao, B. Yu, D. Chen and H. Niu, *ACTA PHYS SIN-CH ED*, 2015, **64**, 028701.